RSC Advances

Suppressing the skin-core structure in injection-molded HDPE parts via the combination of pre-shear and UHMWPE

Zhen Wang[a], Guoqiang Zheng[a,*], Bo Wang[a], Kun Dai[a], John Zhanhu Guo[b], Chuntai Liu[a] , Changyu Shen[a,*]

[a]College of Materials Science and Engineering, The Key Laboratory of Material Processing and Mold of Ministry of Education, Zhengzhou University, Zhengzhou 450001, People's Republic of China

[b]Integrated Composites Laboratory (ICL), Department of Chemical & Biomolecular Engineering, University of Tennessee, Knoxville, TN 37996, USA

Abstract

In this study, pre-shear and ultrahigh molecular weight polyethylene (UHMWPE) were introduced to suppress the skin-core structure of injection-molded high density polyethylene (HDPE) parts. The structural characteristics of injection-molded parts were systematically elucidated through scanning electron microscopy (SEM), two-dimensional wide-angle X-ray diffraction (2D-WAXD) and two-dimensional small-angle X-ray scattering (2D-SAXS). The results showed that oriented lamellae were formed in core region upon pre-shear, and orientation level of oriented lamellae in core region was further enhanced with increasing concentration of UHMWPE.

* Corresponding authors. Tel.: +86 371 63887600.
E-mail address: gqzheng@zzu.edu.cn (G. zheng), shency@zzu.edu.cn (C. Shen).

More interestingly, a much narrowed orientation gap between shear region and core region was obtained if the UHMWPE concentration was increased to 5 wt%. Moreover, crystallinity, long period, and lamellar thickness also increased with increasing UHMWPE concentration upon pre-shear. Naturally, tensile strength of blend parts was promoted due to the narrowed orientation gap between shear region and core region along with enhanced orientation level and increased crystallinity, long period, and lamellar thickness.

Key words: UHMWPE; Pre-shear; Skin-core structure

1. Introduction

The macroscopic properties of polymer products are greatly dependent on the microstructure developed during processing. Therefore, the achievement of high performance property of polymer products through controlling the microstructure has become an important open research subject. It is well known that enhancing the orientation level is a common strategy to improve the mechanical properties[1-3]. Unfortunately, with respect to injection-molded parts, high orientation level can be only obtained in skin region with smaller cross-section area, which could be ascribed to the strong shear stress and high cooling rate. While in core region with larger cross-section area, polymer melt experiences weaker shear stress and lower cooling rate, thus the molecular chains have sufficient time to relax and lead to a lower orientation level. Generally, this inhomogeneous structure, namely skin-core structure, is regarded as a typical structure in injection-molded parts.

As well documented in literatures[4-6], the skin-core structure is not favorable to the improvement of mechanical properties due to the following reasons: on one hand, isotropic crystals in core region goes against the improvement of mechanical properties; on the other hand, owing to the residual stress between the anisotropic skin region and isotropic core region, mechanical properties are deteriorated seriously. From a practical and academic point of view, it is very interesting to enhance the orientation level in core region and thus reduce the difference of orientation level between the skin region and core region. Strategies to suppress the skin-core structure in injection-molded parts include the addition of special additives/fillers and the introduction of intensive shear field[7]. With respect to the former strategy, the addition of special additives/fillers will lower free energy barriers for stretching/orienting molecules[8-10], amplify shear effect[11] or suppress the relaxation of stretched/oriented molecules[12, 13], thus skin-core structure can be largely suppressed. As for the latter strategy, there are many special injection molding technologies which can introduce intensive shear field to suppress the skin-core structure of injection-molded parts such as shear-controlled orientation in injection molding (SCORIM)[14-16], dynamic packing injection molding (DPIM)[17-20], vibration-assisted injection molding (VAIM)[1, 21], push-pull processing[22, 23], *etc*. In a word, the basic principle of aforementioned special injection molding technologies is the application of external shearing fields to the melt during injection/packing stage, promoting molecular alignment. Though skin-core structure can be relieved to a certain degree by these injection molding technologies, the approach of controlling macroscopic shear is complex, because macroscopic shear is supplied by an additional oscillating packing device[7] or axially moved injection-screw[21].

We have designed and built a mixing-injection molding machine recently. This machine can impose shear on melt by a rotating screw during plasticizing process. Interestingly, the pre-sheared melt, showing memory effect, will remarkably change the crystallization kinetics during the subsequent crystallization process, leading to the different crystalline structure[24-26] or formation of oriented structure[27]. Additionally, skin-core structure of injection-molded HDPE parts could be largely relieved through the development of oriented structure in core region[27]. In contrast with these aforementioned special injection molding technologies, this mixing-injection molding machine developed in our laboratory is simple and convenient.

It is well known that long molecular chains are more sensitive to shear and have a significant effect on the subsequent crystallization process and resultant microstructure[28, 29]. Thus, a good understanding of the effect of long molecular chains on the skin-core structure upon pre-shear will give us a valuable guidance on how to manipulate the skin-core structure and resultant properties of injection-molded parts. In this paper, pre-shear was imposed on the melt of HDPE or HDPE/UHMWPE blend during plasticizing process by this mixing-injection molding machine, and the pre-sheared melt was in-situ injected into mold cavity. The results showed that, upon the synergetic effects of pre-shear and UHMWPE, orientation level in core region was enhanced and the skin-core structure was largely suppressed, resulting in an increase of tensile strength in the prepared products.

2. Experimental Section

2.1. Materials and Preparation of Sample

Commercially available HDPE (trade-marked as 5000S) was supplied by Lanzhou Petroleum Chemical Co., China. Its molecular weight (M_w) and melt flow index (MFR) are 3.3×10^5 g/mol and 1.18 g/10 min (190 ^{o}C, 21.6 N), respectively. UHMWPE is supplied by Beijing No. 2 Auxiliary Agent Factory with M_w of 3.0×10^6 g/mol.

HDPE/UHMWPE blend was prepared by a solution blending procedure to ensure that the two phases were intimately mixed at the molecular level[30, 31]. The chosen concentrations of UHMWPE were 2 and 5 wt %, which were significantly higher than the estimated overlap concentration of UHMWPE, 0.3 wt% (the calculation process of the overlap concentration is shown in Supplementary information). The detailed blending procedure was as follows: the powder of UHMWPE was first added into xylene and the mixture was held at 130 ^{o}C under vigorous stirring; after UHMWPE was completely dissolved in xylene (the solution became transparent), HDPE was then added to form a homogeneous solution; at last, the solution was dried and turned into the solid HDPE/UHMWPE blend. In addition, as a reference, pure HDPE was also processed with the same solution blending procedure.

The whole injection molding process could be divided into three procedures and the processing parameters were set as follows. In procedure 1, HDPE or HDPE/UHMWPE blend was put into the barrel and then compressed tightly by a plunger piston driven by a hydraulic system. The barrel temperature was precisely controlled at 180 ^{o}C. In procedure 2, material was melted with the help of the rotating screw. The shear rate applied to melt by the rotating screw was about 16.75 s^{-1} (the calculation process is shown in Supplementary information). In procedure 3, once mixing-plasticization was finished, the melt was in-situ injected into mold cavity. The mold temperature was 50 ^{o}C, and the injection pressure and packing pressure was 75 MPa. In addition, for comparison purpose, the circumferential rotation of the screw was stopped during the plasticizing process to obtain the HDPE part without pre-shear. For brevity, the parts prepared with pre-shear were labeled as PE-Dx, where x represents the concentration of UHMWPE. For example, PE-D2 represents the injection-molded part containing 2 wt% UHMWPE. The part of pure HDPE prepared without pre-shear was named as PE-S0.

2.2. Scanning Electron Microscope (SEM) observation

To evaluate the crystalline morphology, SEM observation was performed. The detailed preparation of specimen for SEM observation is shown in Fig. S3 in Supplementary information. Before SEM observation, the specimens were etched by a solution mixture of 1:1 volume of concentrated sulfuric acid and nitric acid by solving 0.7 wt% of potassium permanganate[25, 27]. The etched surface was first sputter-coated with a layer of gold and then observed by a SEM instrument (JEOL JSM-7500F) operating at 5 kV.

2.3. Two-Dimensional Wide-Angle X-ray Diffraction and Two-Dimensional Small-Angle X-ray Scattering measurements

The crystalline structure and molecular orientation were characterized by Two-Dimensional Wide-Angle X-ray Diffraction (2D-WAXD), which was carried out on a Bruker NanoSTAR-U X-ray radiation source with Cu Ka radiation (1.54 Å) and a beam size with a diameter of 200 µm. The generator was operated at 40 kV and 60 mA.

Two-Dimensional Small-Angle X-ray Scattering (2D-SAXS) experiments were performed at the beamline BL16B1 of the Shanghai Synchrotron Radiation Facility (SSRF) with a wavelength of 0.124 nm and a beam size of 400 µm×600 µm. To collect 2D-SAXS patterns, a Mar CCD detector (2048 × 2048 pixels with pixel size 80 µm) was employed, which was 5235 mm from the samples.

The detailed sample preparation for 2D-WAXD and 2D-SAXS measurements is shown in Fig. S3 in Supplementary information.

2.4. **Tensile test**

Tensile test was carried out according to GB/T1040.2-2006 standard. The test was performed using a universal tensile testing machine (UTM2203, Sun Technology Stock Co., Ltd) with a constant crosshead speed of 50 mm/min and the measured temperature was around 20 ^{o}C. For each condition, the average value reported was derived from at least five tested specimens.

3. Results and Discussion

As fully elucidated in Ref.[32], hierarchical structure of injection-molded parts is generally divided into three regions called skin region, shear region and core region due to the shear and temperature gradients created by the boundary conditions during injection molding process. Generally, the different regions are defined depending on the distance to the skin surface of part[8, 9, 33]. That is, skin region is the outmost region of the injection-molded part, while the region next to skin region is defined as shear region. The center region of part is the core region. However, since the skin region is extremely thin and polymer in this region is considered to be amorphous[8, 33], therefore, we mainly focus our attention on the shear region and core region in this study. In this study, the shear region is at the depth about 200 μm to the skin surface, while core region is at the depth about 1200 μm to the skin surface (the detailed definition of shear region and core region is shown by Fig. S4 and S5 in Supplementary information).

3.1. Crystalline morphology observed by SEM

SEM observation of the etched surface provides morphological information of injection-molded parts. Fig. 1 shows the crystalline morphology of shear and core regions of parts. One can observe a typical skin-core structure in PE-S0, that is, oriented lamellae emerge in shear region (Fig. 1a_1) and isotropic lamellae exist in core region (Fig. 1a_2). Such skin-core structure is mainly attributed to the shear and temperature gradients. During injection molding, melt in shear region experiences strong shear stress and high cooling rate, thus oriented structures (*i.e.* oriented lamellae) are formed. While in core region, the combined effect of weak shear stress and low cooling rate results in a predominantly isotropic lamellae. However, as for PE-D0, it is very interesting to find that shish-kebabs emerge in shear region (Fig. 1b_1) and slightly oriented lamellae exist in core region (Fig. 1b_2). Apparently, pre-shear has a significant effect on facilitating the formation of oriented structures in injection-molded parts, which can be well ascribed to the pre-shear-induced crystallization. Stretched or aligned chains, known as precursors, can be developed along the applied pre-shear flow direction during plasticizing process, which has been confirmed in our previous studies[26, 27]. The growth of precursors in flow direction can lead to the formation of shish, which will induce the epitaxial growth of folded chain lamellae during subsequent crystallization process. Hence, “shish-kebabs” can be observed in shear region of PE-D0. With respect to core region, cooling rate in core region is relatively lower compared with shear region, and thus some precursors formed during plasticizing process will relax to some extent and cannot survive. Therefore, a small amount of oriented lamellae is formed in core region.

However, upon pre-shear, hierarchical structure is remarkably changed if UHMWPE is added. As shown in Fig. 1c_1, c_2, d_1 and d_2, the density of shish-kebab structure in shear region and regularity of lamellar alignment in core region increase compared with those of PE-D0, which should be attributed to the incorporation of UHMWPE. It has been well established that long molecular chains can induce larger number of precursors upon shear, which will participate in the formation of the shish in subsequent crystallization process[20, 34]. In our case, owing to the incorporation of UHMWPE, more long molecular chains will be oriented or extended along the shear direction upon pre-shear and thus more precursors are formed. In addition, the “relatively stable” entanglement points between long molecular chains would be obtained under pre-shear since the concentration of UHMWPE is above the overlapping concentration. Furthermore, these “relatively stable” entanglement points would suppress the relaxation of precursors[35]. Therefore, the precursors have longer relaxation time, which is beneficial to keep the oriented state, leading to occurrence of more oriented structures[36].

However, no shish structure is found in core region of the parts prepared with pre-shear (Fig. 1b_2-d_2), where only oriented lamellae exist. It has been well established that nucleation and growth of oriented lamellae would be impossible if there is no shish structure[37]. Therefore, it can be deduced that shish structure should exist in core region of parts prepared with pre-shear, but it is difficult to be observed by SEM. The invisibility of shish structure can be reasonably attributed to their tiny diameter or volume[38].

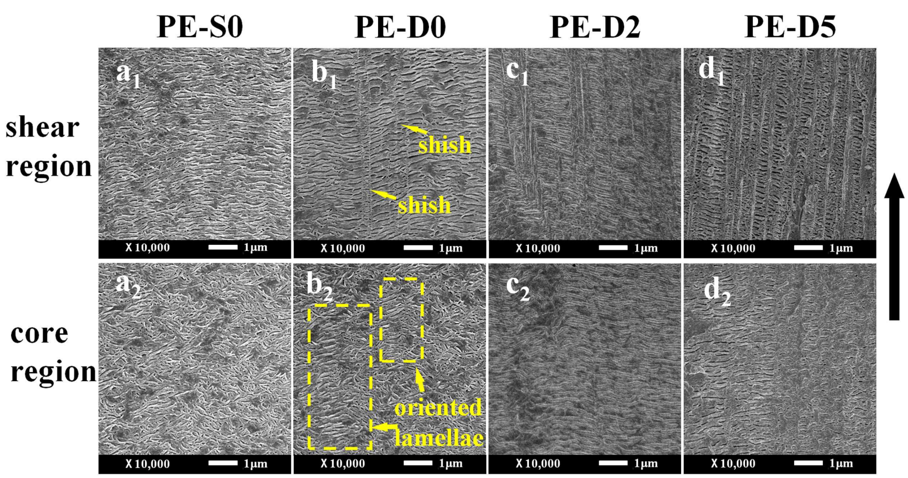

Fig. 1 SEM micrographs of shear region and core region of injection-molded parts. The black arrow represents the melt filling direction.

3.2. Pre-shear-induced orientation

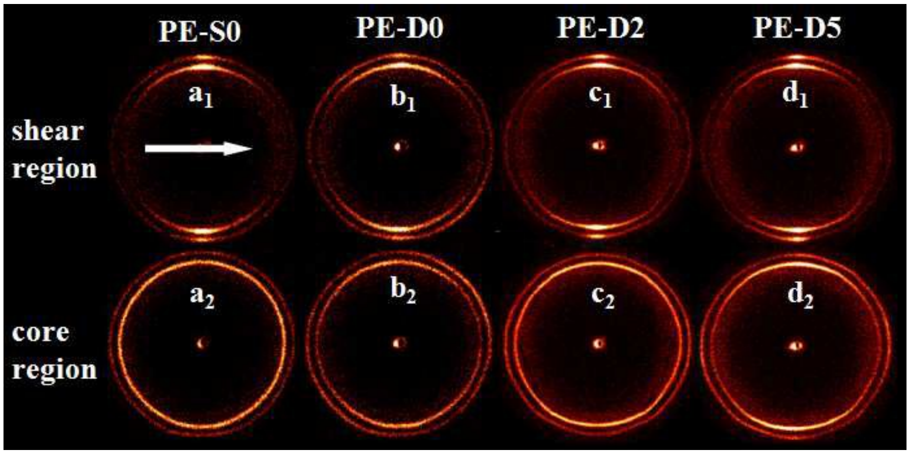

Fig. 2 2D-WAXD patterns of injection-molded parts. The arrow represents the melt filling direction.

2D-WAXD was used to investigate the orientation level and crystallinity of the injection-molded parts. 2D-WAXD patterns of the parts are presented in Fig. 2, where the diffraction reflections from inner to outer circles are assigned to the (110) plane and (200) plane of polyethylene orthorhombic crystals, respectively. For PE-S0, diffraction focused arcs are found in shear region (see Fig. 2a_1), while isotropic circles are observed in core region (see Fig. 2a_2). Clearly, a typical skin-core structure exists in PE-S0, resulting from the shear and temperature gradients. Fig. 2b_1 and b_2 show the 2D-WAXD patterns of PE-D0. It is found that diffraction focused arcs are not only in shear region but also in core region, which indicates the existence of oriented molecular chains in both shear region and core region. Apparently, orientation level in core region is enhanced, which could be attributed to the formation of oriented lamellae induced by pre-shear as mentioned above. In addition, it can be noted that the diffraction focused arcs of core region are sharper in PE-D2 (Fig. 2c_2) and PE-D5 (Fig. 2d_2) compared with that of PE-D0 (see Fig. 2b_2). That is, orientation level in core region increases due to the incorporation of UHMWPE upon pre-shear. This result can be ascribed to the enhancing regularity of lamellar alignment with the incorporation of UHMWPE upon pre-shear.

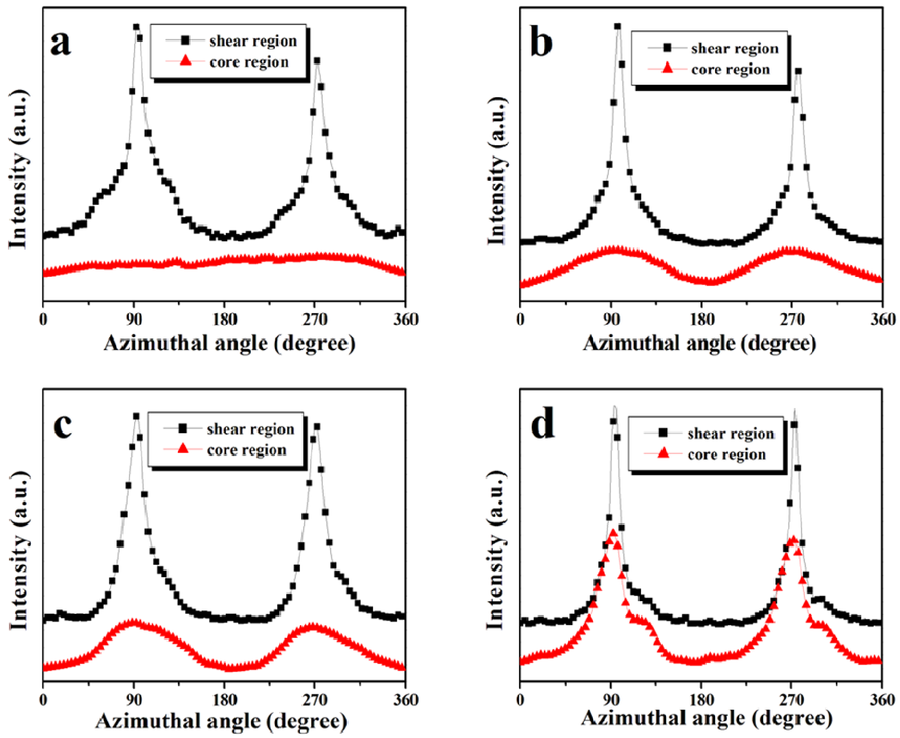

Fig. 3 Intensity distribution of (110) crystal plane of 2D-WAXD along the azimuthal angle from 0 to 360° for PE-S0 (a), PE-D0 (b), PE-D2 (c) and PE-D5 (d).

To quantitatively evaluate the orientation level of injection-molded parts, the (110) intensity distribution along the azimuthal angle from 0 to 360^{o} is presented in Fig. 3. The orientation parameter was calculated using Herman's orientation parameter, which is defined as

$$f_H = \frac{\left(3\langle \cos^2 \phi \rangle - 1\right)}{2} \tag{1}$$

where $\langle \cos^2 \phi \rangle$ is an orientation factor defined as

$$\langle \cos^2 \phi \rangle = \frac{\int_0^{\pi/2} I(\phi)\cos^2\phi \sin\phi \mathrm{d}\phi}{\int_0^{\pi/2} I(\phi)\sin\phi \mathrm{d}\phi} \quad (2)$$

and $I(\phi)$ is the scattering intensity at ϕ, the angle between the normal of a given (hk0) crystal plane and the shear flow direction. To further evaluate the skin-core structure, we defined the orientation parameters of the shear region and core region as f_{shear} and f_{core}, respectively. Δf was defined as the difference of orientation parameters between shear region and core region, which can be calculated by the equation:

$$\Delta f = f_{shear} - f_{core} \quad (3)$$

according to equation (1) and (3), the calculated orientation parameters and the difference of orientation parameters between shear region and core region were calculated and listed in Tab.1.

PE-S0 shows a narrow and high diffraction intensity peak in shear region but no intensity maximum in core region is observed, whose f_{shear} and f_{core} are 0.85 and 0, respectively, with a large Δf of 0.85. Apparently, a highly inhomogeneous structure exists in PE-S0 as observed in most conventional injection-molded parts[39, 40]. In contrast, as for PE-D0, the diffraction intensity peaks can be observed not only in shear region but also in core region, whose orientation parameters are 0.94 (f_{shear}) and 0.30 (f_{core}), with a reduced Δf, 0.64. Therefore, the skin-core structure is relieved to a certain extent for PE-D0 with the application of pre-shear. Interestingly, the diffraction intensity peak of core region in PE-D2 becomes narrower and higher, implying a higher orientation level. As a result, a smaller Δf (0.56) is obtained.

More significantly, PE-D5 exhibits a relatively homogeneous structure whose azimuthal intensity curve of core region become similar with that of shear region, and the orientation parameters are respectively 0.97 (f_{shear}) and 0.82 (f_{core}), with a further decreased Δf , 0.15. These results indicate that the orientation parameter of core region increases with increasing UHMWPE concentration upon pre-shear, and thus the skin-core structure can be further relieved. As mentioned above, the incorporation of UHMWPE will facilitate the formation of precursors, which have long relaxation time. With respect to PE-D5, which has a higher fraction of UHMWPE than PE-D2, more long molecular chains will participate in the formation of precursors, and thus more precursors can be formed. Therefore, more precursors are survived in core region of PE-D5, leading to a higher oriented level than PE-D2. In addition, the blend sample (PE-S5) containing 5 wt% UHMWPE was also prepared without pre-shear. However, the orientation parameter of core region for PE-S5 is very low (i.e., 0.14), leading to a large Δf , 0.82. That is, a highly inhomogeneous structure still exists in PE-S5 (see Fig. S6 and S7 in Supplementary information). In view of this, the skin-core structure of the injection molded HDPE can be substantially relieved upon the synergetic effects of pre-shear and UHMWPE (5 wt%).

Table 1. Orientation parameters of shear and core regions.

Parts	PE-S0	PE-D0	PE-D2	PE-D5
f_{shear}	0.85	0.94	0.91	0.97
f_{core}	0	0.30	0.35	0.82
Δf	0.85	0.64	0.56	0.15

To obtain more quantitative information about the crystalline characteristics, one-dimensional wide-angle X-ray diffraction (1D-WAXD) curves (see Fig. 4a) are obtained from circularly integrated intensity of 2D-WAXD patterns. The overall crystallinity, X_c, was calculated according to the following equation:

$$X_c = \frac{\sum A_{cryst}}{\sum A_{cryst} + \sum A_{amorp}} \tag{4}$$

where A_{cryst} and A_{amorp} are the fitted areas of crystal and amorphous regions, respectively.

As shown in Fig. 4b, crystallinity of shear region is less than that of core region for all parts, which could be ascribed to the temperature gradient in polymer melt injected into mold cavity. That is, the cooling rate in core region is lower than that in shear region, allowing sufficient time for crystallization[41]. For shear region, crystallinity of pure HDPE part prepared with pre-shear is higher than that of pure HDPE part prepared without pre-shear. In other words, once pre-shear was applied, the crystallinity increases from 36.4% of PE-S0 to 38.1% of PE-D0. This result can be explained by pre-shear-induced crystallization. In our case, precursors generated by pre-shear will behave as oriented nuclei, leading to a high nucleation density and speeding up crystallization process[42-44]. Furthermore, once UHMWPE is incorporated, crystallinity of shear region increases to 41.2% for PE-D2, and 43.4% for PE-D5. As mentioned above, the incorporation of UHMWPE will further facilitate the formation of precursors, thus a higher nucleation density is obtained and the crystallization process is further enhanced. Therefore, it is understandable that the crystallinity increases with increasing UHMWPE concentration with the help of pre-shear. However, for core region, crystallinity is slightly increased upon the application of pre-shear and the incorporation of UHMWPE, which may be attributed to the sufficient crystallization time caused by lower cooling rate.

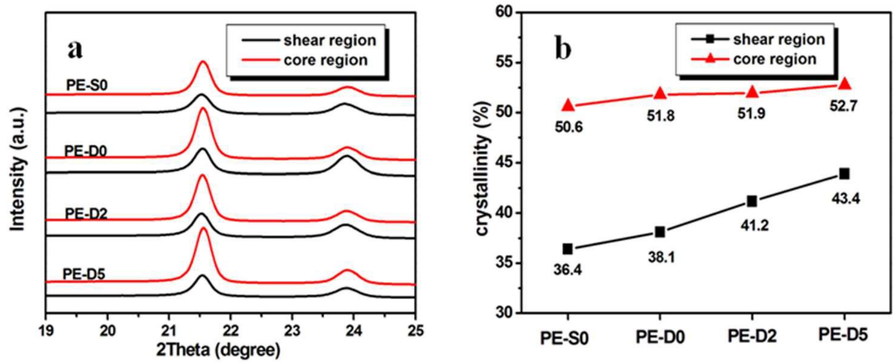

Fig. 4 1D-WAXD curves (a) and crystallinity (b) of injection-molded parts.

To analyze the crystalline lamellae arrangement in the injection-molded parts, 2D-SAXS measurements have been conducted. Fig.5 shows the 2D-SAXS patterns of both shear and core regions of the parts. Clearly, scattering streaks in meridional direction emerge in shear regions of all parts, implying the existence of shish structure parallel to the flow direction. Moreover, the equatorial scattering maxima appears in shear regions of all parts, indicating the existence of oriented lamellae in these regions[45, 46]. Therefore, shish-kebab structure is formed in shear regions of all parts, which is consistent with most conventional injection-molded parts. With respect to the core region, equatorial scattering maxima is absent in PE-S0 (Fig. 5a_2), while it exists in PE-D0 (Fig. 5b_2), which is indicative of absence of oriented lamellae in core region of PE-S0 and existence of oriented lamellae in core region of PE-D0. This result is well consistent with the SEM observation and our previous study[27], which can be attributed to the introduction of pre-shear. Furthermore, under the same applied pre-shear condition, the equatorial scattering intensity of core region increases with increasing UHMWPE concentration (Fig. 5c_2 and d_2), which is indicative of increasing regularity of oriented lamellae[46]. Clearly, coupling with the pre-shear during plasticizing process, the presence of UHMWPE will further facilitate the formation of more oriented structure in core region. In addition, weak scattering streaks in meridional direction, indicating the existence of shish structure, can be also observed in Fig. 5b$_2$-d$_2$. In light of this, a conclusion can be safely obtained that shish-kebab structure is also formed in core region of parts prepared with pre-shear. To the best of our knowledge, this observation has been seldom reported so far[47].

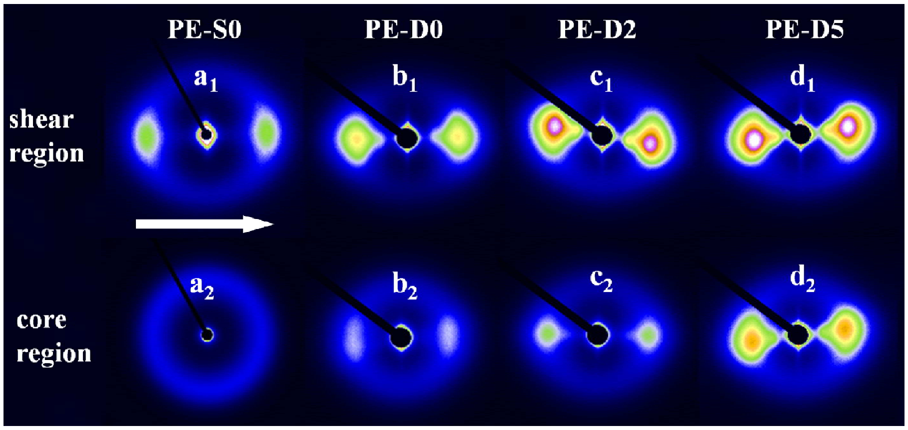

Fig. 5 2D-SAXS patterns of injection-molded parts. The arrow represents the melt filling direction.

For quantitative comparison, azimuthal scans of 2D-SAXS (Fig. 6) were derived from Fig. 5 to calculate orientation degree according to equation (1). The detailed orientation parameters are listed in Tab. 2. As for PE-S0, orientation parameters are 0.57 (f_{shear}) and 0 (f_{core}), with a large Δf, 0.57. However, once pre-shear is applied (PE-D0), the case changes. f_{shear} and f_{core} are 0.65 and 0.23 respectively, leading to a lower Δf (0.42) compared with PE-S0. Apparently, the skin-core structure in PE-D0 is relived slightly, which should be ascribed to the application of pre-shear[27]. Moreover, the incorporation of UHMWPE leads to a further decrease in Δf. For instance, a decreased Δf , 0.24, is obtained in PE-D2. What is interesting is that Δf become very small, 0.07, when the UHMWPE concentration is 5 wt% (*i.e.,* PE-D5). This result once again indicates clearly the significance of UHMWPE in the suppression of skin-core structure upon pre-shear.

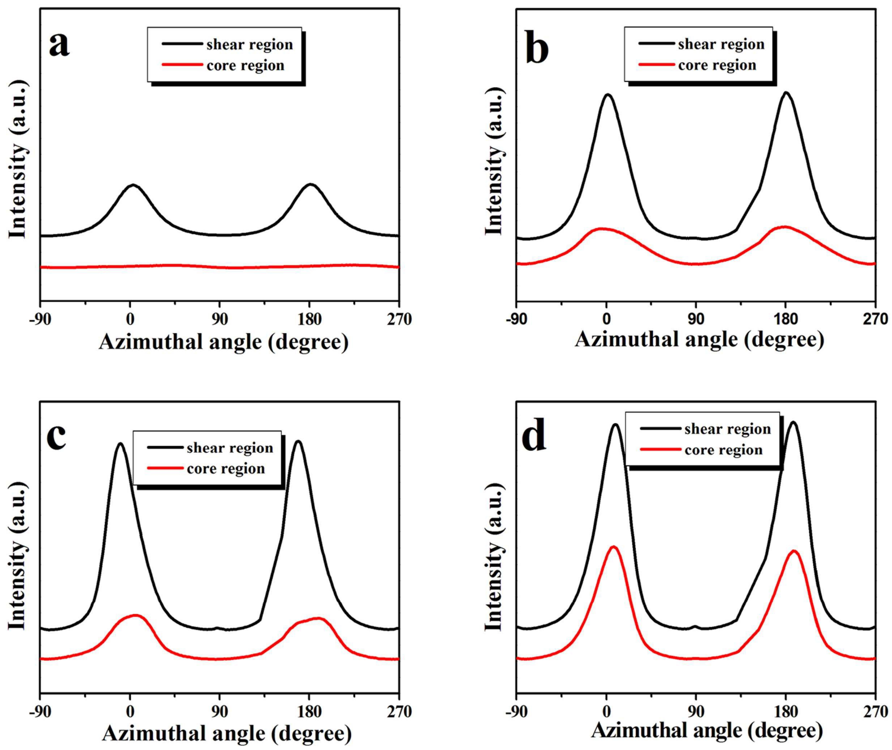

Fig. 6 Intensity distribution of 2D-SAXS along the azimuthal angle from -90 to 270° for PE-S0 (a), PE-D0 (b), PE-D2 (c) and PE-D5 (d).

Table 2. Corresponding orientation parameters of shear and core region.

Parts	PE-S0	PE-D0	PE-D2	PE-D5
f_{shear}	0.57	0.65	0.73	0.75
f_{core}	0	0.23	0.49	0.68
Δf	0.57	0.42	0.24	0.07

From the measured 2D-SAXS intensity, one-dimensional correlation function (Strobl method) $K(z)$ is calculated by cosine Fourier transformation[48]

$$K(z) = \frac{1}{r_e^2 (2\pi)^3} \int_0^\infty cos(qz) 4\pi q^2 \sum(q) dq \qquad (5)$$

where q is the scattering vector $q = 4\pi \sin\theta_B / \lambda$ (θ_B denotes the Bragg angle), $\sum(q)$ the differential cross section per unit volume, and r_e the classical electron radius. Fig. 7 shows the one-dimensional correlation function $K(z)$ for the lamellar stacks obtained from 2D-SAXS patterns. According to the $K(z)$ curve, the long period can be obtained from the position of the first maximum. The lamellar thickness can be determined from the baseline of the first minimum and the tangent line shown in Fig.7c[48].

It has been well established that the long period of oriented crystallites is generally larger than that of the isotropic ones[49, 50]. Thus, it is understandable that long period (Fig. 8a) in both shear region and core region of PE-D0 is slightly larger than that of PE-S0. Moreover, the long period in shear region and core region further increase with increasing UHMWPE concentration, which could be ascribed to the development of more oriented structures. At the same time, it should be noted that the increase in lamellar thickness (Fig. 8b) is also consistent with the increased long period. In our case, crystallization process is speeded up upon pre-shear, resulting in thicker and more perfect crystals. Therefore, it is reasonable that lamellar thickness in shear region and core region of PE-D0 is larger than that of PE-S0. Moreover, incorporation of UHMWPE will further enhance crystallization process upon pre-shear. Thus, it is reasonable that lamellar thickness in both shear region and core region increases with the increasing concentration of UHMWPE. In addition, it should be noted that both long period and lamellar thickness of core region are larger than those of shear region. This should be ascribed to the low cooling rate in core region[51].

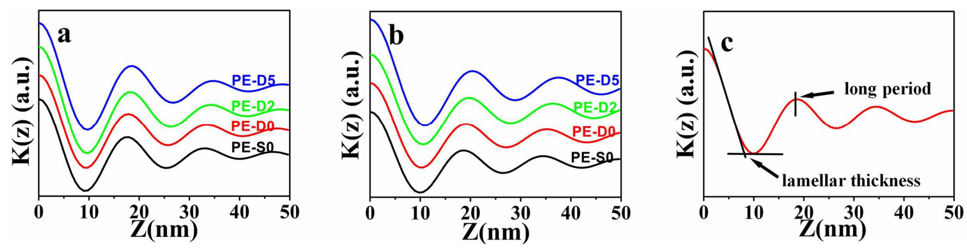

Fig. 7 One-dimensional correlation function $K(z)$ of shear region (a) and core region (b) obtained from 2D-SAXS patterns. The calculation method (c) of long period and lamellar thickness obtained from the one-dimensional correlation function $K(z)$.

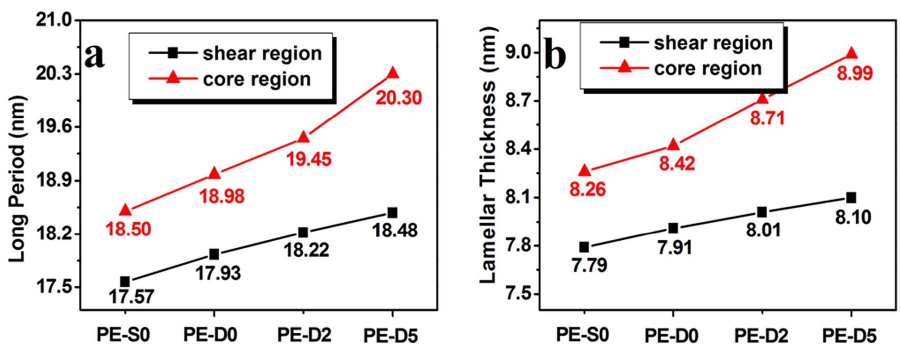

Fig. 8 The long period (a) and lamellar thickness (b) of injection-molded parts.

3.3. Tensile properties

Since different crystalline structures have been obtained in these parts, we are very curious whether such different structure can lead to different mechanical properties. Fig. 9 shows the representative stress-strain curves of as-prepared parts. Clearly, tensile strength has no obvious change between PE-S0 (24.8 ± 0.39 MPa) and PE-D0 (24.4 ± 0.31 MPa) no matter whether pre-shear was applied or not. This result can be explained as follows: although the application of pre-shear has enhanced the orientation level in core region to a certain extent, the difference of orientation level between shear region and core region is still large, which shows negative effect on enhancing tensile strength. As for the blend parts, however, an obvious increase in tensile strength is obtained. That is, adding 2 wt% UHMWPE achieves 23% increase of the tensile strength (30.5 ± 0.76 MPa) vs. PE-S0. When UHMWPE loading is increased to 5 wt%, tensile strength of the PE-D5 is 38.8 ± 1.79 MPa, representing a 56% increase over PE-S0. The increase of tensile strength should result from the synergetic effects of pre-shear and UHMWPE. According to the aforementioned results, orientation level in core region is enhanced with increasing UHMWPE concentration upon pre-shear. Consequently, the difference of orientation level between shear region and core region is reduced and internal stress is further eliminated. In addition, as mentioned above, crystallinity, long period, and lamellar thickness, all increase due to the synergetic effects of pre-shear and UHMWPE. These crystalline paramenters play important roles in determining tensile properties[52-54]. Reasonably, such suppression of skin-core structure, along with high orientation level in core region and increased crystallinity, long period, and lamellar thickness, leads to an improvement in tensile strength of blend parts.

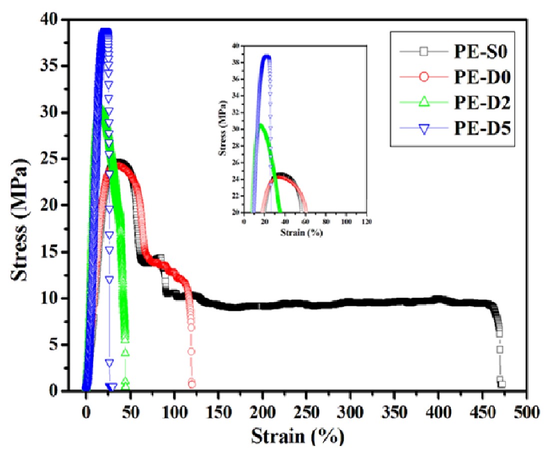

Fig. 9 Representative stress-strain curves of injection-molded parts.

4. Conclusions

In this study, the skin-core structure of the injection-molded HDPE is largely relieved by the synergetic effects of application of pre-shear during plasticizing process and incorporation of UHMWPE. Oriented precursors induced by the pre-shear, which can survive in the melt, will facilitate the formation of oriented structures and enhance the orientation level in core region of injection-molded HDPE. Moreover, the incorporation of UHMWPE will further facilitate the formation of more precursors upon pre-shear, and thus more oriented structures are formed and the orientation level is further enhanced in core region. In addition, crystallinity, long period, and lamellar thickness also increase upon pre-shear, and further increase with increasing UHMWPE concentration. The suppression of skin-core structure together with enhanced orientation level in core region and increased crystallinity, long period, and lamellar thickness, leads to a promotion in tensile strength of injection-molded parts.

Acknowledgment

We gratefully acknowledge the financial support of this work by National Natural Science Foundation of China (51173171, 11172271). We also express thanks to Plan for Scientific Innovation Talent of Henan Province and Opening Project of State Key Laboratory of Polymer Materials Engineering (Sichuan University).

References

1. Y. B. Li, Y. H. Liao, X. Q. Gao, Y. Yi, W. T. Ke and K. Z. Shen, *J. Polym. Sci. Part. B: Polym. Phys.*, 2005, **43**, 13-21.

2. X. Y. Qian, H. Liu, F. H. Liu, X. Q. Gao and J. Zhang, *J. Appl. Polym. Sci.*, 2012, **123**, 682-690.

3. K. Wang, F. Chen, Q. Zhang and Q. Fu, *Polymer*, 2008, **49**, 4745-4755.

4. J. Kubáut, J. A . Månson and M. Rigdahl, *Polym. Eng. Sci.*, 1983, **23**, 877-882.

5. G. Kalay, R. A. Sousa, R. L. Reis, A. M. Cunha and M. J. Bevis, *J. Appl. Polym. Sci.*, 1999, **73**, 2473-2483.

6. B. A. G. Schrauwen, L. C. A. Von Breemen, A. B. Spoelstra, L. E. Govaert, G. W. M. Peters and H. E. H. Meijer, *Macromolecules*, 2004, **37**, 8618-8633.

7. K. Wang, F. Chen, Z. Li and Q. Fu, *Prog. Polym. Sci.*, 2014, **39**, 891-920.

8. P. W. Zhu and G. Edward, *Macromolecules*, 2004, **37**, 2658-2660.

9. P. W. Zhu, J. Tung and G. Edward, *Polymer*, 2005, **46**, 10960-10969.

10. P. W. Zhu, A. Phillips, J. Tung and G. Edward, *J. Appl. Phys.*, 2005, **97,** 104908.

11. B. Yalcin, D. Valladares and M. Cakmak, *Polymer*, 2003, **44**, 6913-6925.

12. T. Fu, Y. Zhang, J. Zhang, T. Wang and X. Gao, *J. Macromol. Sci. Part B: Phys.*, 2014, **53**, 861-877.

13. Z. Zhao, Q. Yang, M. Kong, D. Tang, Q. Chen, Y. Liu, F. Lou, Y. Huang and X. Liao, *RSC Adv.*, 2015, **5**, 43571-43580.

14. C. I. Ogbonna, G. Kalay, P. S. Allan and M. J. Bevis, *J. Appl. Polym. Sci.*, 1995, **58**, 2131-2135.

15. S. Ghosh, J. C. Viana, R. L. Reis and J. F. Mano, *Mater. Sci. Eng. A.*, 2008, **490**, 81-89.

16. G. Kalay and M. J. Bevis, *J. Polym. Sci. Part. B Polym. Phys.*, 1997, **35**, 415-430.

17. G. Zhong, L. Li, E. Mendes, D. Byelov, Q. Fu and Z. Li, *Macromolecules*, 2006, **39**,

6771-6775.

18. X. Yi, C. Chen, G. Zhong, L. Xu, J. Tang, X. Ji, B. S. Hsiao and Z. Li, *J. Phys. Chem. B.*, 2011, **115**, 7497-7504.

19. Y. Chen, Z. Huang, Z. Li, J. Tang and B. S. Hsiao, *RSC Adv.*, 2014, **4**, 14766-14776.

20. W. Cao, K. Wang, Q. Zhang, R. Du and Q. Fu, *Polymer*, 2006, **47**, 6857-6867.

21. A. Kikuchi, J. P. Coulter and R. R. Gomatam, *J. Appl. Polym. Sci.*, 2006, **99**, 2603-2613.

22. K. Waschitschek, A. Kech and J. D. Christiansen, *Composites. Part A*, 2002, **33**, 735-744.

23. D. E. Smith, D. A. Tortorelli and C. L. Tucker III, *Comput. Meth. Appl. Mech. Eng.*, 1998, **167**, 325-344.

24. C. Ji, M. Xie, B. Chang, K. Dai, B. Wang, G. Zheng, C. Liu and C. Shen, *Composites. Part A*, 2013, **46**, 26-33.

25. M. Xie, B. Chang, H. Liu, K. Dai, G. Zheng, C. Liu, C. Shen and J. Chen, *Polym. Compos.*, 2013, **34**, 1250-1260.

26. B. Chang, M. Xie, K. Dai, G. Zheng, S. Wang, C. Liu, J. Chen and C. Shen, *Polym. Test.*, 2013, **32**, 545-552.

27. L. Huang, Z. Wang, G. Zheng, J. Z. Guo, K. Dai and C. Liu, *Mater. Des.*, 2015, **78**, 12-18.

28. A. Elmoumni, H. H. Winter and A. J. Waddon, *Macromolecules*, 2003, **36**, 6453-6461.

29. C. Hadinata, C. Gabriel, M. Ruellman and H. M. Laun, *J. Rheol.*, 2005, **49**, 327-349.

30. Y. Huang, J. Xu, J. Li, B. He, L. Xu and Z. Li, *Biomaterials*, 2014, **35**, 6687-6697.

31. L. Yang, R. H. Somani, I. Sics, B. S. Hsiao, R. Kolb, H. Fruitwala and C. Ong, *Macromolecules*, 2004, **37**, 4845-4859.

32. S. Fellahi, B. D. Favis and B. Fisa, *Polymer*, 1995, **37**, 2615-2626.

33. P. W. Zhu, J. Tung, A. Phillips and G. Edward, *Macromolecules,* 2006, ***39***,1821-1831.

34. R. H. Somani, L. Yang and B. S. Hsiao, *Polymer*, 2006, **47**, 5657-5668.

35. L. Xu, Y. Huang, J. Xu, X. Ji and Z. Li, *RSC Adv.*, 2014, **4**, 1512-1520.

36. A. Nogales, B. S. Hsiao, R. H. Somani, S. Srinivas, A. H. Tsou, F. J. Balta-Calleja and T. A. Ezquerra, *Polymer*, 2001, **42**, 5247-5256.

37. G. Kumaraswamy, R. K. Verma, A. M. Issaian, P. Wang, J. A. Kornfield, F. Yeh, B. S. Hsiao and R. H. Olley, *Polymer*, 2000, **41**, 8931-8940.

38. S. Liang, K. Wang, C. Tang, Q. Zhang, R. Du and Q. Fua, *J. Chem. Phys.*, 2008, **128,** 174902.

39. S. Liparoti, A. Sorrentino, G. Guzman, M. Cakmak and G. Titomanlio, *RSC Adv.*, 2015, **5**, 36434-36448.

40. J. Cao, K. Wang, W. Cao, Q. Zhang, R. Du and Q. Fu, *J. Appl. Polym. Sci.*, 2009, **112**, 1104-1113.

41. L. Wang, M. Yang, Q. Zhang, R. Zhang, J. Wu and J. Feng, *Polym. Adv. Technol.*, 2013, **24**, 541-550.

42. J. Zhu, M. Li, R. Rogers, W. Meyer, R. Ottewill, W. Russel and P. Chaikin, *Nature*, 1997, **387**, 883-885.

43. N. Chan, M. Chen, X. Hao, T. A. Smith and D. E. Dunstan, *J. Phys. Chem. Lett.*, 2010, **1**, 1912-1916.

44. D. Lellinger, G. Floudas and I. Alig, *Polymer*, 2003, **44**, 5759-5769.

45. R. H. Somani, L. Yang, B. S. Hsiao, P. K. Agarwal, H. A. Fruitwala and A. H. Tsou, *Macromolecules*, 2002, **35**, 9096-9104.

46. M. Fujiyama, T. Wakino and Y. Kawasaki, *J. Appl. Polym. Sci.*, 1988, **35**, 29-49.

47. H. R. Yang, J. Lei, L. B. Li, Q. Fu and Z. M. Li, *Macromolecules*, 2012, **45**, 6600-6610.

48. G. R. Strobl and M. Schneider, *J. Polym. Sci. Polym. Phys. Ed.*, 1980, **18**, 1343-1359.

49. Y. H. Chen, Y. M. Mao, Z. M. Li and B. S. Hsiao, *Macromolecules*, 2010, **43**, 6760-6771.

50. R. H. Somani, B. S. Hsiao, A. Nogales, H. Fruitwala, S. Srinivas and A. H. Tsou, *Macromolecules*, 2001, **34**, 5902-5909.

51. L. Wang and M. Yang, *RSC Adv*, 2014, **4**, 25135-25147.

52. F. Mai, K. Wang, M. Yao, H. Deng, F. Chen and Q. Fu, *J. Phys. Chem. B.,* 2010, **114**, 10693-10702.

53. B. Pukánszky, I. Mudra and P. Staniek, *J. Vinyl. Addit. Technol.*, 1997, **3**, 53-57.

54. Y. Gao, K. Ren, N. Ning, Q. Fu, K. Wang and Q. Zhang, *Polymer*, 2012, **53**, 2792-2801.

Figure Captions

Fig. 1 SEM micrographs of shear region and core region of injection-molded parts. The black arrow represents the melt filling direction.

Fig. 2 2D-WAXD patterns of injection-molded parts. The arrow representsthe melt filling direction.

Fig. 3 Intensity distribution of (110) crystal plane of 2D-WAXD along the azimuthal angle from 0 to 360° for PE-S0 (a), PE-D0 (b), PE-D2 (c) and PE-D5 (d).

Fig. 4 1D-WAXD curves (a) and crystallinity (b) of injection-molded parts.

Fig. 5 2D-SAXS patterns of injection-molded parts. The arrow represents the melt filling direction.

Fig. 6 Intensity distribution of 2D-SAXS along the azimuthal angle from -90 to 270° for PE-S0 (a), PE-D0 (b), PE-D2 (c) and PE-D5 (d).

Fig. 7 One-dimensional correlation function $K(z)$ of shear region (a) and core region (b) obtained from 2D-SAXS patterns. The calculation method (c) of long period and lamellar thickness obtained from the one-dimensional correlation function $K(z)$.

Fig. 8 The long period (a) and lamellar thickness (b) of injection-molded parts.

Fig. 9 Representative stress-strain curves of injection-molded parts.

Tables

Table 1. Orientation parameters of shear and core regions.

Parts	PE-S0	PE-D0	PE-D2	PE-D5
f_{shear}	0.85	0.94	0.91	0.97
f_{core}	0	0.30	0.35	0.82
Δf	0.85	0.64	0.56	0.15

Table 2. Corresponding orientation parameters of shear and core region.

Parts	PE-S0	PE-D0	PE-D2	PE-D5
f_{shear}	0.57	0.65	0.73	0.75
f_{core}	0	0.23	0.49	0.68
Δf	0.57	0.42	0.24	0.07